Available online at www.sciencedirect.com
SCIENCE DIRECT®
Polymer 45 (2004) 2483–2493
polymer
www.elsevier.com/locate/polymer

Epoxy resin cured with diamine bearing azobenzene group

Ewa Schab-Balcerzak[a,*], Henryk Janeczek[a], Bożena Kaczmarczyk[a], Henryk Bednarski[a], Danuta Sęk[a], Andrzej Miniewicz[b]

[a]*Centre of Polymer Chemistry, Polish Academy of Sciences 34 M., Curie-Skłodowska Str., 41-819 Zabrze, Poland*
[b]*Institute of Physical and Theoretical Chemistry, Wrocław University of Technology, 50-370 Wrocław, Poland*

Received 10 November 2003; received in revised form 2 February 2004; accepted 5 February 2004

Abstract

The epoxy resin: *N,N*-diglycidyl-4-glycidyloxyaniline (DGOA) is cured with the new diamine-chromophore: 2,4-diamino-4′-methylazobenzene (DMAB). The spectral characterization of infrared spectroscopy (FTIR), ^{1}H NMR spectroscopy and of elemental analysis (EA), confirm the chromophore structure. The curing kinetics of aminophenol epoxy resin/2,4-diamino-4′-methylazobenzene system is studied in isothermal experiments by means of differential scanning calorimetry (DSC). The structural changes occurring during the cure reaction are investigated by Fourier transform infrared spectroscopy (FTIR). Thermal stability characterized by the temperature of 5 and 10% weight loss and residue at 1000 °C of the cured product is studied by thermogravimetric analysis (TGA). Amorphous character of the cured material is determined using X-ray spectroscopy. The preliminary investigations of optical grating recording are carried out.

Keywords: Epoxy resins; Cure reaction kinetics; Photoresponsive chromophores

1. Introduction

Thermoset epoxy composites are most often used in high-performance applications because of their unique properties. Epoxy resins generally possess excellent characteristics: heat, moisture and chemical resistance, toughness, electrical and mechanical resistance, and good adhesion to many substrates. The versatility of their properties result in wide range of applications for surface coatings, adhesives, painting materials, composites, laminates, encapsulates for semiconductors, insulating materials for electric devices [1,2]. Moreover, the epoxy composites find new and new possibilities of applications, particularly when azobenzene chromophores are introduced in epoxy system. Polymers containing azobenzene units are of special interest with respect to the reversibility of the photoorientation. The main aim of research on this kind of polymers is their utilization for optical information storage, information processing, optical switching devices and diffractive optical element, among others. Over the last few years, epoxy-based polymers attracted much attention as materials for opto-electronic (optical) applications. Epoxy resins containing azobenzene chromophore were investigated from the point of view of application in holography [3–7] and for other second-order nonlinear optical processes [8]. In most cases epoxy resin based on diglycidyl ether of bisphenol A cured with various amino functional azobenzene chromophore were utilized for holographic gratings.

The epoxy resins are characterized by the presence of the oxirane group,

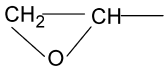

which is able to react with compounds possessing active hydrogen atoms, including amines, amides [9]. It is well known that the cure of thermoset resins involves conversion of liquid monomers into three-dimensional network. Properties of a cured epoxy polymer are generally dependent on the chemical structure of epoxy resin and the curing agent. The curing conditions are next factor, which determines physical and mechanical properties. The knowledge of the curing kinetics: kinetic rate and how the rate changes with cure temperature are important and useful for predicting the chemical conversion achieved after a cure schedule. Curing

* Corresponding author.
E-mail address: ewabalce@server.cchp-pan.zabrze.pl (E. Schab-Balcerzak).

0032-3861/$ - see front matter © 2004 Elsevier Ltd. All rights reserved.
doi:10.1016/j.polymer.2004.02.027

kinetics of epoxy resin can be studied with different techniques but differential scanning calorimetry (DSC) is the most powerful method [10,11]. The curing reaction of epoxy resins is highly exothermic. The review of literature shows that curing kinetics of the epoxy-amine system was studied mostly in isothermal conditions. It is well experimentally justified that prior to vitrification the reaction is only kinetically controlled. After vitrification (when glass transition temperature T_g of the material rises beyond the cure temperature T_c) the diffusion of the chain segments can become a dominant factor. When the epoxy resin polymerizes at the temperatures below the glass transition temperature, the curing reaction does not reach complete conversion. 100% conversion is only possible at reaction temperature equal to or greater than T_g temperature [13]. The first stage of curing, chemically controlled is an autocatalyzed reaction and is well described by the model proposed by Kamal [12,14]. Horie et al. considered this chemical controlled region to be the third-order reaction [10]. The effect of diffusion control can be incorporated into the reaction kinetics by modifying the overall rate constant. During the course of isothermal curing, both in the kinetically and diffusion-controlled regimes, the overall rate constant is assumed to be a combination of the chemical and diffusion rate constants [15].

The glass transition temperature T_g considerably increasing with the changes in chemical conversion regardless of the cure path can be a practical parameter for investigation of the cure process [16]. According to the reported results both theoretical and empirical T_g increases linearly [11,14] or nonlinearly [15–18] with conversion. It was found that there exists one-to-one relationship between T_g and conversion, independent of cure temperature [15–19].

The present paper deals with the new epoxy system with azoaromatic groups included in the backbone chain. New photoresponsive chromophore-2,4-diamino-4′-methylazobenzene, which has not been described in the literature yet, is utilized as curing agent.

This paper consist of four parts, in the first one the investigations of structural changes during curing are presented, the second is devoted to kinetics study and in the next one relationship between glass transition temperature and the rate of conversion and time of curing is discussed, the last concerns preliminary investigations of holography grating recording in the obtained new material.

2. Experimental

2.1. Materials

p-Toluidine (Aldrich), 1,3-phenylenediamine (Aldrich) and *N*,*N*-diglycidyl-4-glycidyloxyaniline (Aldrich) are used as received. The primary diamine (curing agent): 2,4-diamino-4′-methylazobenzene has been synthesized.

2.1.1. Synthesis and characteristic of 2,4-diamino-4′-methylazobenzene

2.7 ml of concentrated hydrochloric acid and 10 ml of water have been added to 10 mmol of *p*-toluidine to obtain salt solution. Then a solution of 10 mmol of sodium nitrite in 1.5 ml of water has been added dropwise to the cooled salt solution (ice bath) and the mixture has been stirred at a temperature between 0 and 5 °C during 15 min. Then it has been poured slowly into a solution containing 10 mmol of 1,3-phenylenediamine in 8 ml of methanol. The reaction has been carried out for 30 min in ice bath and neutralised with sodium acetate to pH 5–6. After rising the temperature to 20 °C the mixture has been stirred for 1 h. The product has been filtered, washed with water and dried in vacuum at 70 °C (90% yield).

^{1}H NMR (DMSO-d_6, ppm): $\delta = 2.41$ (d, CH_3, 3H), 5.58 (s, NH_2, 2H), 5.91 (d, ArH, 1H), 6.02 (d, d, ArH, 1H), 6.74 (s, NH_2, 2H), 7.23 (d, ArH, 2H), 7.38 (d, ArH, 1H), 7.57 (d, ArH, 2H), UV–vis (*m*-cresol): $\lambda_{max} = 437$, 285 nm, ($C_{13}H_{14}N_4$) (226.28): Calcd: C 69.00, H 6.24, N 24.76; Found: C 68.92, H 6.27, N 24.70, Mp: 141 °C.

2.1.2. Curing route and characteristic of epoxy-based polymer used for optical properties study

A sample of *N*,*N*-diglycidyl-4-glycidyloxyaniline/2,4-diamino-4′-methylazobenzene (DGOA/DMAB) mixed homogeneously in a molar ratio 1:1.5. X-ray spectroscopy confirmed amorphous nature of the cured resin. Thermal stability of the cured resin has been investigated by TGA. It has lost 5 and 10% of weight at 270 and 300 °C, respectively. The residue at 800 °C is 36%.

2.2. Measurements

^{1}H NMR spectra have been run on a Varian Inova 300 Spectrometer in DMSO-d_6. UV spectra have been recorded in DMA solution on BECKMAN Acta M-IV spectrophotometer within the 200–3300 nm range. X-ray diffraction patterns have been performed at room temperature using a conventional θ–2θ diffractometer and Ni-filter Cu Kα X-ray in the reflection mode. Thermogravimetric (TG) analyses have been performed on a Paulik-Erdey apparatus at a heating rate of 10 °C/min under nitrogen. For elemental analysis a 240C Perkin–Elmer analyzer is used. The holography grating was recorded using 514.5 and 488 nm Ar^+ laser light. The gratings formed in the polymer film were monitored by measuring the power of the first-order diffracted beam. The recording light powers were $P_{01} = 12.6$, $P_{02} = 25.3$ mW in case of laser light Ar^+ 514.5 nm (beam intersection angle $\theta = 5.9°$) and $P_0 = 6.05$ and 13.5 mW for laser light 488 nm.

2.2.1. FTIR measurements

Infrared spectra are acquired on a BIO-RAD FTS-40A Fourier transform infrared spectrometer in the range of 4000–400 cm^{-1} at a resolution of 2 cm^{-1} and for

accumulated 64 scans. The investigated samples are in the form of solid films obtained from solutions in $CHCl_3$ (evaporation of the solvent has been carried out at room temperature). The spectra recorded at elevated temperatures are obtained using Carl Zeiss Jena high-temperature control equipment in the temperature range from 20 to 240 °C. The samples are heated under nitrogen at the rate of 1 °C/min and FTIR spectra have been recorded at 10 °C.

2.2.2. DSC measurements

DSC measurements are done using a TA DSC 2010 apparatus. The cure of the resins is studied under both dynamic and isothermal conditions. Approximately 25 mg samples of DGOA and curing agent DMAB (molar ratio 1:1.5) in aluminium pan are used for measurements.

3. Result and discussion

The reaction between epoxides and amines occurs in two significant stages: primary amine reacts with an epoxide usually yielding a secondary amine which in turn reacts with another epoxide resulting in a tertiary amine as the final product.

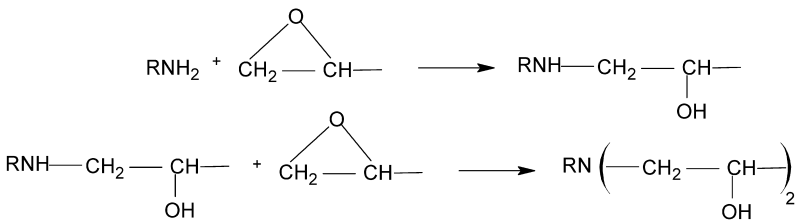

Both reactions were found to be catalysed by the hydroxy groups formed during the reaction. The reactivities of primary and secondary amines with epoxide may be different as shown in the literature [17]. Horie et al. proposed the following scheme to describe the overall kinetics of the epoxide reaction with primary amine [20]:

$$A_1 + E + (HX)_a \rightarrow A_2 + (HX)_a + (HX)_a$$

$$A_1 + E + (HX)_0 \rightarrow A_2 + (HX)_0 + (HX)_a$$

$$A_2 + E + (HX)_a \rightarrow A_3 + (HX)_a + (HX)_a$$

$$A_2 + E + (HX)_0 \rightarrow A_3 + (HX)_0 + (HX)_a$$

where A_1, A_2 and A_3 are primary, secondary, and tertiary amines; E is the epoxide group; $(HX)_a$ is the hydroxyl group of the reaction products; and $(HX)_0$ is the initial hydroxyl resident.

In this work we have studied the influence of curing conditions on the kinetics of the process and on the glass transition temperature of the resin using epoxy resin and diamine as a curing agent as presented in Scheme 1. Infrared spectroscopy and calorimetric method are applied for the study.

3.1. FTIR study of curing reaction

The assignment of particular bands at the infrared spectra of pure *N,N′*-diglycidyl-4-glycidyloxyaniline (DGOA) and 2,4-diamino-4′-methylazobenzene (DMAB) are shown in Table 1.

In the IR spectrum of DGOA a weak broad band with maximum at 3480 cm^{-1} ascribed to stretching vibrations of O–H groups is seen. This indicates that in DGOA some epoxy rings have been already opened. In the spectrum obtained after mixing both compounds, considerable shifts of the bands in the region of 3600–3100 cm^{-1} take place (Fig. 1).

The bands attributed to stretching vibrations of NH_2 groups at 3397 and 3309 cm^{-1} shift to 3451 and 3370 cm^{-1}, respectively. These changes can be explained as the results of breaking of intermolecular hydrogen bonds occurring in

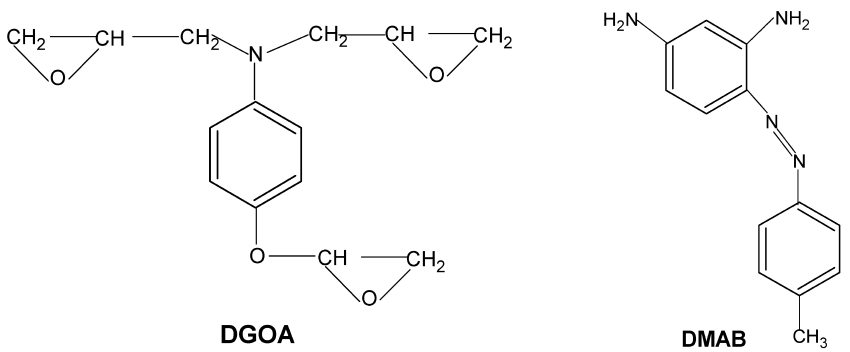

Scheme 1. Chemical structures of *N,N*-diglycidyl-4-glycidyloxyaniline (DGOA) and 2,4-diamino-4′-methylazobenzene (DMAB).

Table 1
Wavenumbers (cm^{-1}) and assignment of IR bands of DGOA and DMAB

DGOA	Approximate assignment	DMAB	Approximate assignment
3480	ν O–H	3397	ν_a NH_2
3053	ν CH (Ph)	3309	ν_s NH_2
2996	ν_s CH_2 (R)	3060	ν CH (Ph)
2922	ν_a CH_2	3022	ν CH (Ph)
2874	ν_s CH_2	2942	ν_a CH_3
1615	ν Ph	2913	ν_a CH_3
1578	ν Ph	2855	ν_s CH_3
1514	ν Ph	1618	δ NH_2
156	ν Ph + δ CH_2	1602 sh	ν Ph
1425	δ CH_2 (–O)	1568	ν Ph
1411	δ CH (R)	1550	ν N=N
1385		1500	ν Ph
1344	ω CH_2	1472	δ_a CH_3 + ν Ph
1300 sh	ν Ph	1417	δ_a CH_3
1239	ν R + τ CH_2 + δ CH_2	1385	δ_s CH_3
1191	ν_a NC_2	1330	ν Ph
1154 sh	δ CH Ph	1303	ν Ph
1132	ν C–C	1287	δ CH (Ph)
1077	ν C–O (Ph) + ν C–C	1235	
1039	δ CH (Ph)	1221	
973	γ CH (Ph)	1183	δ CH (Ph)
940	δ_a R	1127	δ CH (Ph)
909	δ_s R	1041	ρ Me + ρ NH_2
821	ρ CH_2 + γ CH (Ph)	973	ρ Me
766	γ CH (Ph)	955	γ CH (Ph)
754	γ CH (Ph)	849	γ CH (Ph)
722	γ Ph	827	γ CH (Ph)
563		805	γ CH (Ph)
525		639	δ Ph + ω NH_2
		599	γ Ph
		533	γ Ph
		521	δ Ph
		462	δ Ph + γ Ph
		420	δ Ph

Ph, phenyl ring; Me, methyl group; R, epoxy ring; ν, stretching vibrations; a, antisymmetric; s-symmetric; δ, in plane deformation; ρ, rocking vibrations; ω, wagging vibrations; τ, twisting vibrations; γ, out-of-plane deformation; sh, shoulder, ass, associated.

amines in the condensed phase. This effect is similar to those of solution diluting.

Relatively smaller shifts of the bands from 1568 to 1584 cm^{-1} and from 1550 to 1574 cm^{-1} ascribed to stretching vibrations of phenyl ring and N=N groups, respectively, are observed and may indicate interactions between the two components and breaking of hydrogen bonds in the amine. The rest of the spectrum is the sum of the spectra of particular components.

To detect the changes in FTIR spectrum caused by the reaction run, samples are heated under nitrogen at the rate of 1°/min and FTIR spectra are recorded by every 10 °C. In our investigations we have taken into consideration especially these bands the changes in intensities and positions of which correspond to the course of reaction, i.e. the bands characteristic for vibrations of $-NH_2$ amine and epoxy groups.

The changes in areas of the bands in the region of 922–878 cm^{-1} due to symmetric in plane deformation vibrations of epoxy ring have been chosen as the most representative to the quantitative study of the run of the reaction.

Fig. 2 shows spectra of the reaction mixture, i.e. epoxy resin and diamine recorded at different temperatures. As Fig. 2 indicates the area of the band in the range of 922–878 cm^{-1} decreases continuously and at 190 °C reaches zero. However, further heating to 240 °C causes lowering of the baseline in the analyzed region. It can suggest that a small amount of epoxy groups, not detected by the method used, remain yet at 190 °C and react during further heating to 240 °C. In the range from 150 to 180 °C the quickest decrease in this area is observed (Fig. 2(b)).

Similar changes in the areas of the band at 2996 cm^{-1} characteristic for stretching vibrations of CH_2 epoxy group during the heating are observed. However, their quantitative studies are not possible due to the overlapping by a stronger band ascribed to the stretching vibration of CH_2 groups (Fig. 3(a)).

During the heating of the mixture several changes in the region from 3600 to 3100 cm^{-1} are also noticed (Fig. 3(a)). The bands at 3451 and 3370 cm^{-1} disappear due to the stretching vibrations of NH_2 groups with a simultaneous appearance and increase in intensities of bands at about 3560 and 3470 cm^{-1}. It can be interpreted as stretching vibrations of free and associated O–H group, respectively. However, the bands due to the stretching vibration of NH groups of secondary amines appear in that region as well. Overlapping of the analyzed bands makes that region difficult to look into. Consequently at 190 °C broad band with shoulders at 3560, 3475 and 3408 cm^{-1} ascribed to free, associated –OH groups and =NH groups in secondary amine, respectively, is seen in that region. Further heating to 240 °C causes only a slight decrease in intensity of the band at about 3408 cm^{-1}, which confirms the fact that a little amount of secondary amine and epoxy groups were condensed till heating to 240 °C.

These changes are accompanied by the decrease in area of the band at about 1618 cm^{-1} (Fig. 3(b)). This band is a sum of the bands corresponding to the deformation vibrations of $-NH_2$ groups and stretching vibrations of phenyl ring. Simultaneously a shoulder at about 1590 cm^{-1} appears. This band can be ascribed to the deformation vibrations of NH groups in secondary amine. During heating to 240 °C the shoulder disappears and a band with maximum at 1610 cm^{-1} due to stretching vibrations of phenyl ring is recorded. It is also a proof that during heating to 240 °C further cross-linking takes place.

Likewise in the region of 1400–700 cm^{-1} changes in the spectra correspond to the emerging secondary and tertiary amine groups and the OH group (Fig. 3(b)). However, these bands completely overlap and are difficult to investigate, particularly as far as the observed changes are concerned.

Further heating to 240 °C causes the appearance of a low intensity band at 505 cm^{-1}, which can be ascribed to the

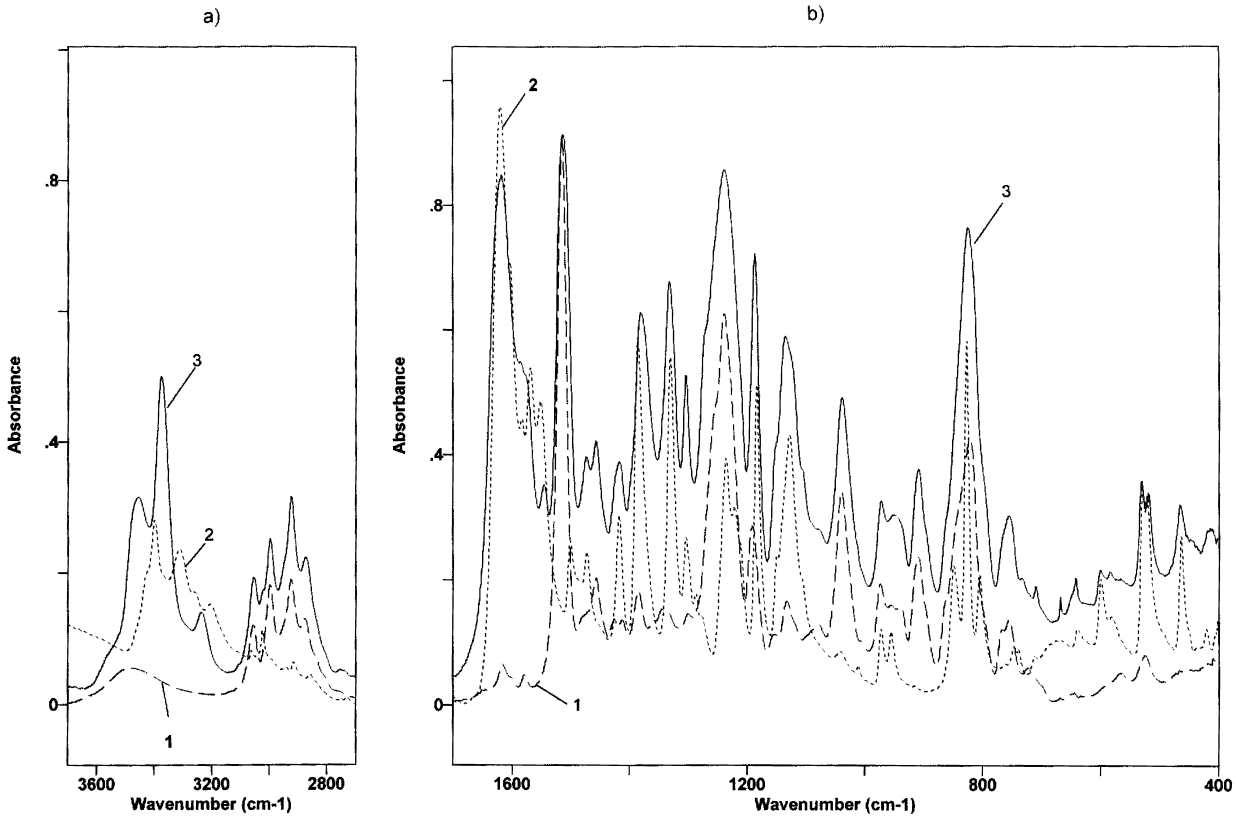

Fig. 1. FTIR spectra of DGOA (1), DMAB (2) and mixture of them (3) in the region of 3700–2700 cm^{-1} (a) and 1700–400 cm^{-1} (b).

deformation vibration of C–N group in tertiary amine [21]. After cooling to room temperature only the changes in the region of 3700–3200 cm^{-1} are noticed (Fig. 4).

The increase in intensity of the band at 3408 cm^{-1} characteristic for stretching vibrations of associated O–H groups indicates the hydrogen bonds forming after the cooling.

3.2. Kinetics of epoxide reaction with diamine

The curing reaction of epoxy resin (DGOA) with DMAB has been carried out isothermally in DSC apparatus at the following temperatures: 130, 140, 150, 160, 165, 170, 180 and 190 °C. The reaction is considered complete when the DSC curve levels down to the baseline. The total area under the exothermal curve, based on the extrapolated baseline at the end of the reaction, is used to calculate the isothermal heat of cure, ΔH_i, at a given temperature. Typical DSC curve for this reaction at temperature 140 °C is shown in Fig. 5 as an example.

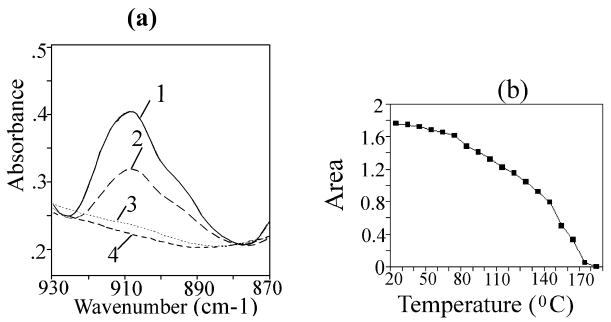

Fig. 2. (a) FTIR spectra of reaction mixture in the region of 930–870 cm^{-1} at 20 (1), 140 (2), 190 (3) and 240 °C (4). (b) Changes of area of band in the region of 922–878 cm^{-1} during heating.

The data obtained at the beginning of the test are not very reliable because of the stabilization period while the sample introduced into instrument was reaching the desired temperature. Therefore, up to the time of about 180 s, the interpolated values of data have been taken into account. After each isothermal run, the sample is cooled to 20 °C and then reheated at the rate of 20 °C/min to 300 °C to determine the residual heat of the reaction, ΔH_R (Fig. 5(b)). The total heat evolved during the curing reaction is $\Delta H_T = \Delta H_i + \Delta H_R$.

The values of isothermal and residual heat of the reaction are collected in Table 2. It can be seen that the residual heat of the reaction H_R is decreasing along with the increase of the cure temperature T_c. The value of total heat of the reaction H_T for these tests is comparable to H_T obtained from the dynamic tests where sample is heated at the rate of 20 °C/min and is equal to 783 J/g.

The chemical conversion α, which is given by $\alpha = H_i/H_T$, is the basic parameter influencing the properties of the cured material. In order to predict the chemical conversion reached after the cure schedule it is useful to know the kinetic rate and how the rate changes with the cure

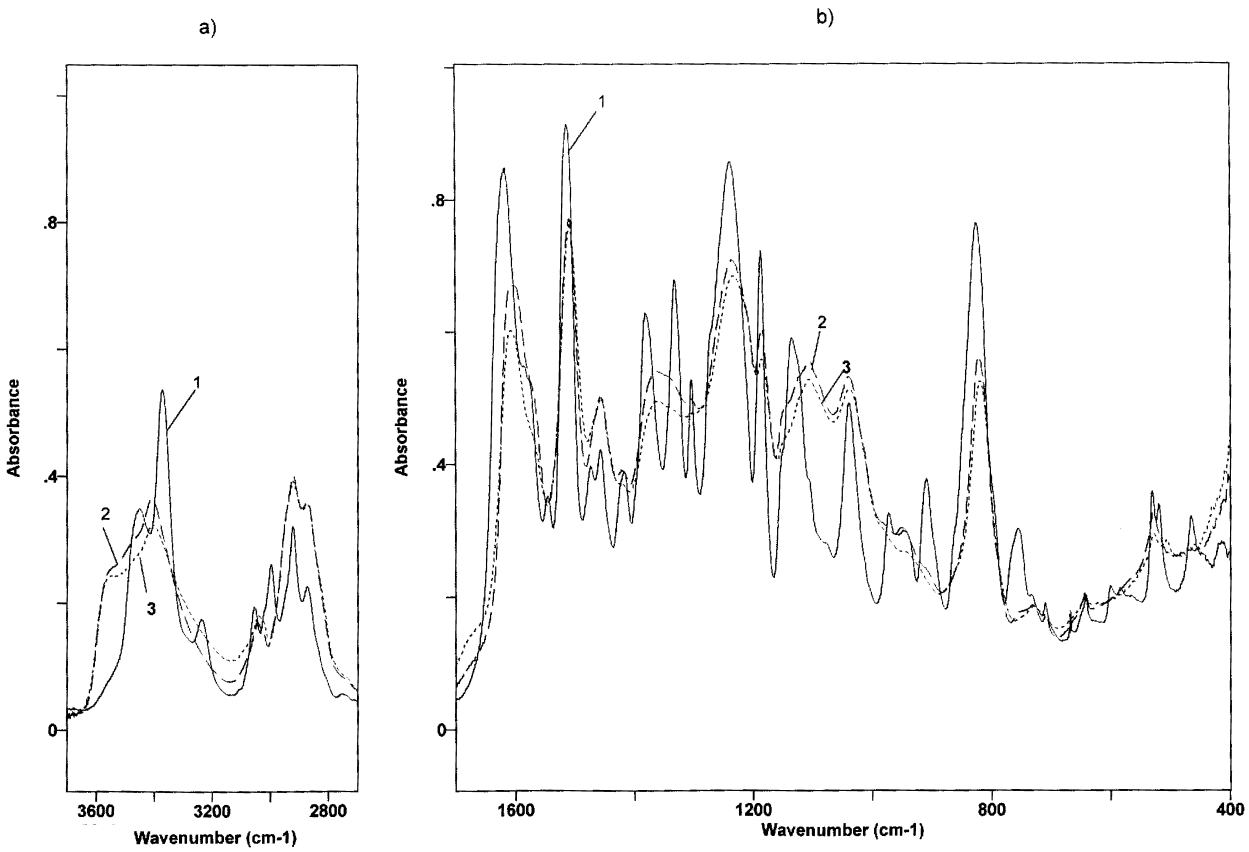

Fig. 3. FTIR spectra of reaction mixture at 20 (1), 190 (2) and 240 °C (3), in the region of 3700–2700 cm^{-1} (a) and 1700–400 cm^{-1} (b).

temperature. The heat released during the curing is proportional to the extent of the reaction, in turn the reaction rate, $d\alpha/dt$, is proportional to the heat flow, dH/dt [12,14]. The rate of reaction as a function of time has been calculated from the rate of heat flow measured in isothermal DSC experiments:

$$\frac{d\alpha}{dt} = \frac{1}{H_T}\frac{dH_i}{dt}, \quad (1)$$

A series of isothermal reaction rate curves (obtained from DSC measurements), as a function of time, is presented in Fig. 6.

Taking these curves into account a few dependences can be observed. The reaction rate increases rapidly because of the autoacceleration and reaches a maximum. After this point it starts to decrease and gradually dies out. The increase in temperature of the curing reaction influences the value of the reaction rate at the maximum. The peak of the reaction rate becomes higher and shifts to a shorter time along with the increasing T_c. The plot shows the maximum

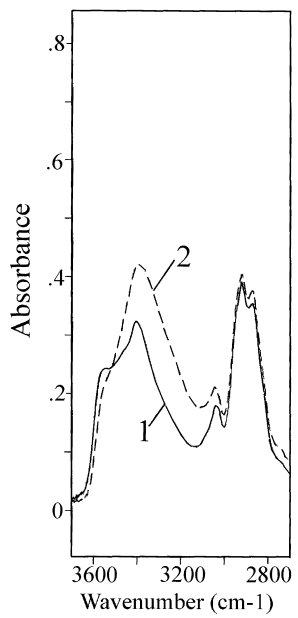

Fig. 4. FTIR spectra of reaction mixture at 240 °C (1) and after cooling to room temperature (2) in the region of 3700–2700 cm^{-1}.

Table 2
Heat of reaction in isothermal and dynamic DSC tests

T_c (0°C)	H_i (J/g)	H_R (J/g)	$H_T = H_i + H_R$ (J/g)
130	488	257	745
140	551	219	769
150	569	187	756
160	625	131	756
165	611	119	730
170	598	88	686
180	752	20	777
190	836	–	836

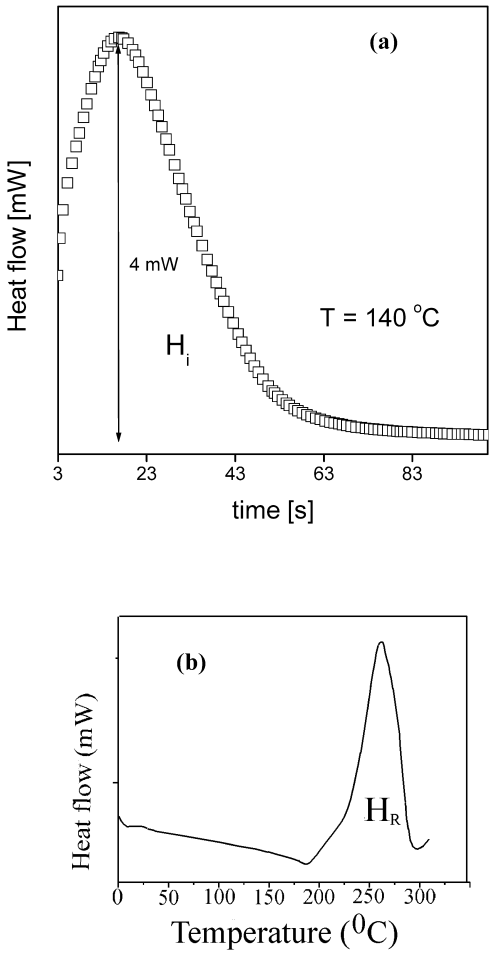

Fig. 5. DSC curve for DGOA/DMAB system: (a) isothermal measurement at 140 °C, (b) dynamic measurement (heating rate 20 °C/min) after isothermal measurement.

in the $d\alpha/dt$ versus time-curve at $t \neq 0$, which is characteristic for autocatalytic reactions [11,14]. By partial integration of areas under the experimental curves in Fig. 6, the fractional conversion as a function of time has been

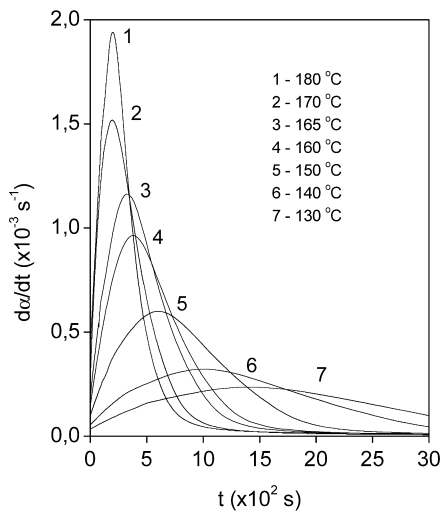

Fig. 6. Isothermal reaction rate as a function of time at different T_cs.

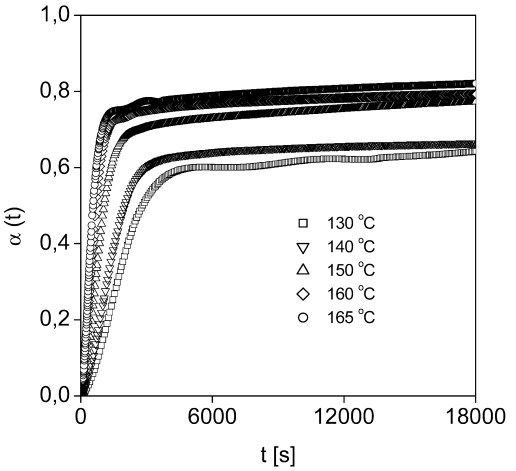

Fig. 7. Isothermal fractional conversion as a function of time at different T_cs.

obtained. Fig. 7 presents the plot of curing reaction conversion (calculated from the experimental data) versus time at different isothermal temperatures.

Initially, the conversion level increases with time and finally approaches a limiting conversion. The higher the curing temperatures the higher the limiting fractional conversion is reached. This is to be expected since in step polymerisation the original monomer disappears early in the reaction and after the gel point most of reactive functional groups are attached to the cross-linked network. Flory predicted that a cross-linked system will gel molecularly when its fractional conversion, α, reaches a constant critical values $\alpha_{gel} = 0.58$ for the reaction of bifunctional unit with an equivalent amount of tetrafunctional unit [13].

As mentioned above, the maximum reaction rate is at $t > 0$, which excludes simple nth-order kinetics. Therefore, in this work Kamal's model (describing the chemically controlled cure), arising from the autocatalytic reaction mechanism is applied to our isothermal data. Kamal proposed the following expression [12]:

$$\frac{d\alpha}{dt} = (k_1 + k_2\alpha^m)(1-\alpha)^n, \tag{2}$$

where m and n are the reaction orders, and k_1, k_2 are the rate parameters which are functions of temperature. Non-linear regression analysis is used for the computation of the parameters: m, n and k_2, while the reaction rate constant k_1 was determined as the initial reaction rate at $t = 0$. The comparison of the data calculated form equilibrium (2) with the experimental ones presents Fig. 8 as an example.

As expected, at later stages of the reaction one cannot observe good correlation between the experimental data and the calculated ones. There are significant discrepancies in the traces of curves. The differences reveal because of the diffusion effect, which can become even a dominating factor. Truthfulness of this observation may be easy verified, as it is well known that the onset of diffusion is expected to appear at vitrification when $T_g = T_c$. For

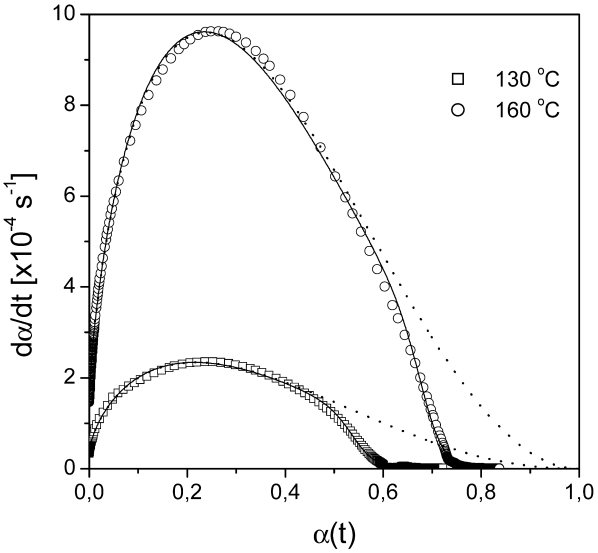

Fig. 8. Comparison of calculated data from Kamal eq. (solid line) with experimental data (symbols).

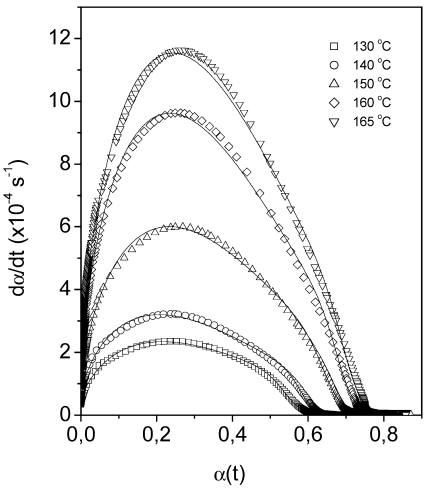

Fig. 9. Comparison of calculated data included the diffusion effect (solid line) with experimental (symbols).

instance, in our case this condition is experimentally fulfilled at 130 °C for $\alpha = 0.506$ thus, in vicinity of the point where departure of corresponding curve from the experimental data really takes place (see Fig. 8). In order to describe the diffusion effect the following semiempirical equation proposed by Chern and Poehlein is applied [22]:

$$k_d = k_c \exp(-C(\alpha - \alpha_c)), \tag{3}$$

where k_c is the rate constant for non-diffusion-controlled (chemical) kinetics, α_c is a certain critical value of α at which $k_d = k_c$ and C is a constant [22]. According to Rabinowitch [23] the overall effective rate constant k_{eff} can be expressed as follows:

$$\frac{1}{k_{eff}} = \frac{1}{k_d} + \frac{1}{k_c} \tag{4}$$

Now, adequate change of names of introduced parameters (k_c in Eqs. (3) and (4) on k_2 and k_2 in Eq. (2) on k_{eff}) allows for incorporation of the diffusion effect into Kamal's equation. Finally, resulting expression for the overall reaction rate can be written as:

$$\frac{d\alpha}{dt} = (k_1 + k_2\alpha^m)(1-\alpha)^n \frac{1}{1 + \exp[C(\alpha - \alpha_c)]} \tag{5}$$

The comparison of the best fitted, to Eq. (5), curves with the corresponding experimental data is shown in Fig. 9.

Fig. 9 clearly shows that Eq. (5) leads to a very good description of the experimental data in the whole range of α.

The resulting values of the kinetic parameters obtained from Eq. (5) for isothermal tests are collected in Table 3.

As seen in Table 3 the parameters k_1 and k_2 increase with T_c, whereas the total reaction order, $m + n$, slightly decreases with T_c. The tendency to an overall reaction order 3 is confirmed [13]. The ratio of the reaction rate constants k_1/k_2 is about 0.035 and to good extend independent of the reaction temperature.

As seen from Table 3 the parameters k_1 and k_2 depend on the temperature. For a kinetically controlled reaction mechanism, the temperature dependence of the rate constant is given by the Arrhenius relationship:

$$k_i = A_i \exp(-E_i/RT) \quad i = 1, 2 \tag{6}$$

where A_i is the pre-exponential constant, E_i is the activation energy, R is the gas constant, and T is the absolute temperature. The relationship between ln k_i and reciprocal temperature $1/T$ is shown in Fig. 10.

Linear dependency allows for the determination of activation energy from the slope of straight line. The activation energies E_1 and E_2 are 71.6 and 70.5 kJ/mol, respectively.

At the end this section it is worth examining more exactly the ratio of the overall effective rate constant k_{eff} to the chemical rate constant known as the diffusion factor $f(\alpha)$ which with help of Eqs. (3) and (4) can be written as:

$$f(\alpha) = \frac{k_{eff}}{k_c} = \frac{1}{1 + \exp[C(\alpha - \alpha_c)]} \tag{7}$$

Table 3
Kinetic parameters for isothermal curing of DGOA/DMAB with parameters for the diffusion

Parameter	T_c (°C)				
	130	140	150	160	165
k_1 ($\times 10^{-4}$)	0.346	0.544	0.997	1.467	1.890
k_2 ($\times 10^{-3}$)	1.054	1.489	2.638	4.418	5.272
k_1/k_2	0.033	0.036	0.037	0.033	0.036
m	0.680	0.690	0.704	0.719	0.733
n	2.265	2.386	2.088	2.142	2.081
$m + n$	2.945	3.076	2.792	2.861	2.814
α_c	0.545	0.586	0.652	0.688	0.704
C	40.9	49.4	38.3	41.3	37.9

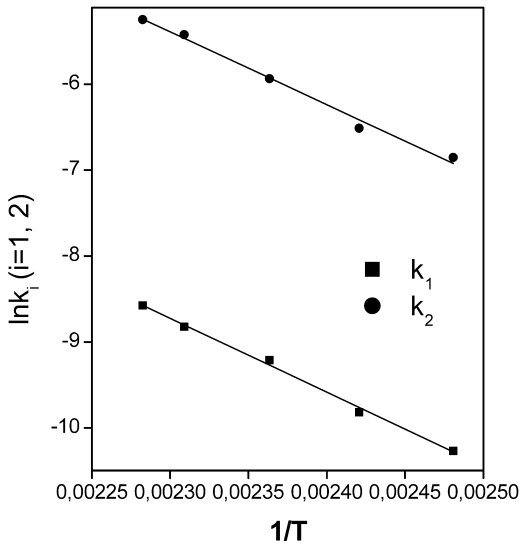

Fig. 10. Arrhenius plot of curing reaction rate constants k_1 and k_2.

The plot of $f(\alpha)$ versus α at different T_c is presented in Fig. 11.

As illustrated in Fig. 11, for $\alpha \ll \alpha_c$, $f(\alpha)$ is approximately equal to 1 and diffusion effect is negligible. When α approaches α_c, $f(\alpha)$ begins to decrease and for $\alpha \gg \alpha_c$ reaches zero, which indicates discontinuation of the reaction.

3.3. Glass transition temperature and curing process

One-to-one relationship between T_g and the degree of the cure was reported [12,16]. In our work in order to determine the glass transition temperature T_g as a function of fractional conversion, series of samples are cured in the DSC cell at 130, 140 and 155 °C for various periods of time. Each of the

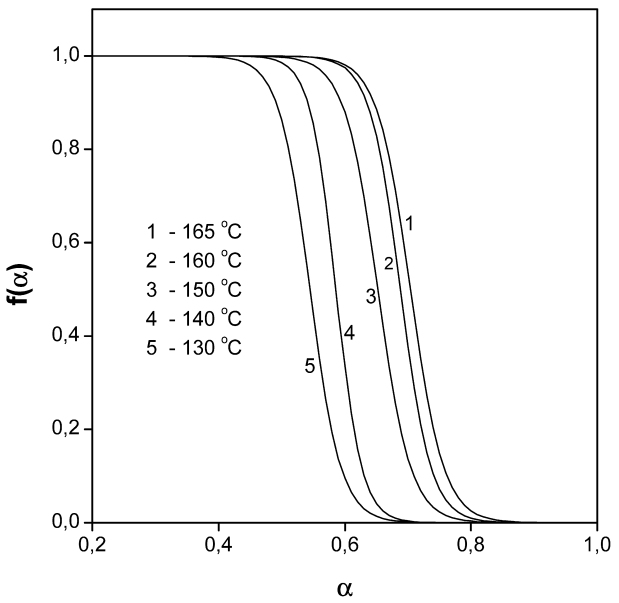

Fig. 11. $f(\alpha)$ versus α at various temperatures of isothermal heating.

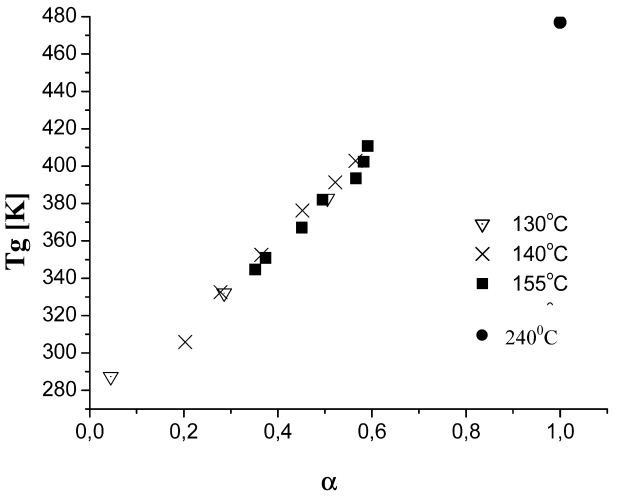

Fig. 12. Glass transition temperature of partially cured material at different T_cs versus the corresponding fractional conversion.

samples heated isothermally (partially cured) are cooled rapidly to 0 °C and then reheated at 20 °C/min to 240 °C to determine the glass transition temperature and the residual heat of the reaction. T_g is taken as the midpoint of the step transition. The corresponding fractional conversion is calculated.

Glass transition temperatures as a function of conversion are shown in Fig. 12.

$T_g = 204$ °C has been determined by DSC for the sample previously heated at 240 °C during 118 h. Achieving 100% conversion in such a highly cross-linked system is in itself difficult and because of it the $T_{g,inf}$ probably will be higher than determined 204 °C.

The correlation between fractional conversion α and values of T_g at different curing temperatures T_c is good and is independent from the temperature cure path. T_g increases linearly up to α about 1.

3.4. Optical grating recording experiments

The presence of azobenzene groups in the polymer should enable reversible optical grating recording due to photoisomerisation initiated processes leading to either photoinduced optical anisotropy or relief formation due to mass transport. Preliminary holographic grating recording experiments have been carried out in the film prepared from cured epoxy resin (DGOA/DMAB). Kinetics of holographic grating recording in film has been studied using a standard two-wave mixing technique [24]. Diffraction gratings have been recorded in two cases: when two incoming beams I_1 and I_2 are linearly polarised with electric field vectors perpendicular to the incidence plane—so called VV-polarisation (also ss) and second case when the two beams are orthogonally polarised with respect to each other—so called VH-polarisation (sp). In both cases (VV and VH) of polarisation geometry a periodic birefringence and/or dichroism is induced. This results in a diffraction grating

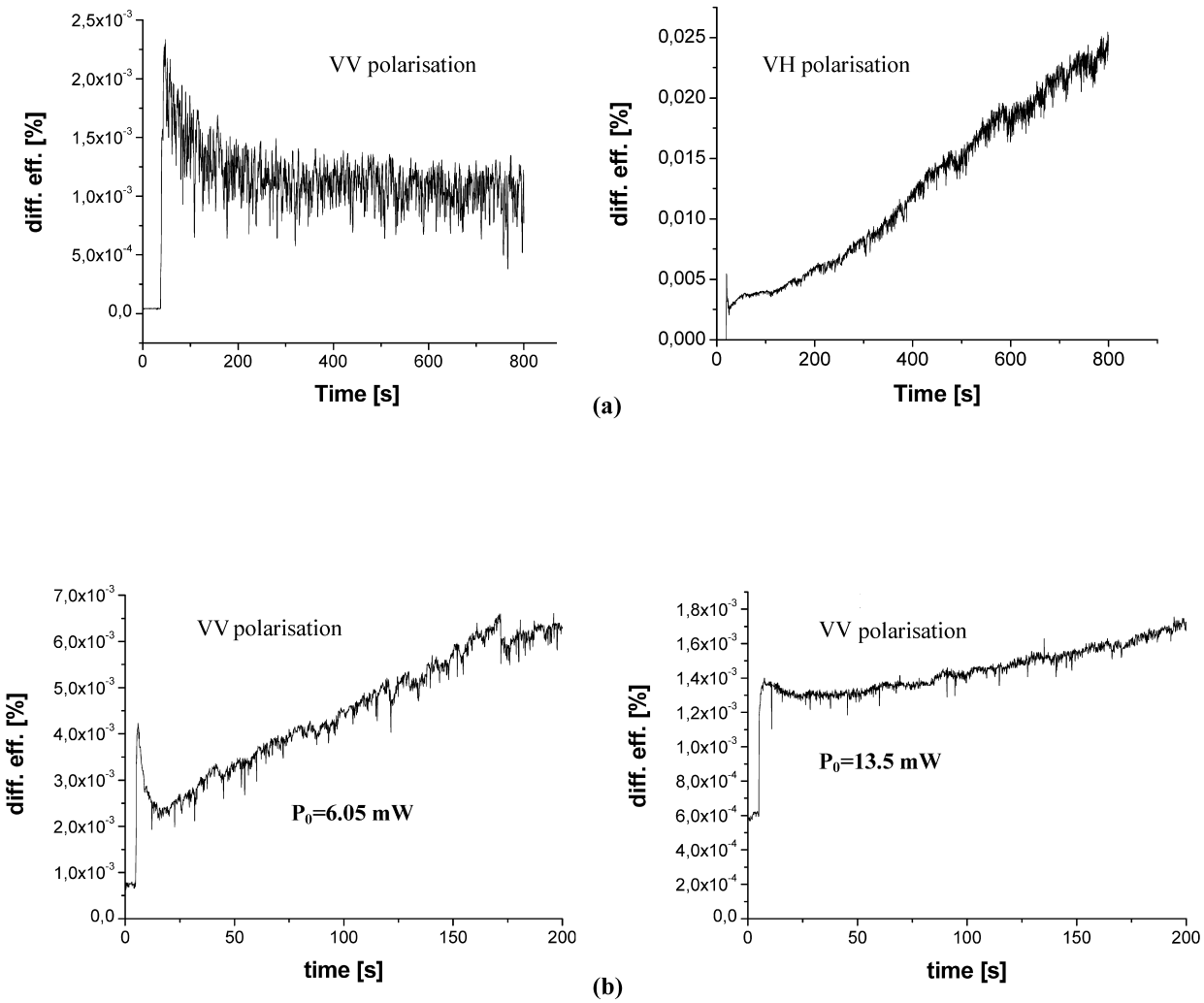

Fig. 13. Kinetics of holographic grating recording in thin films of DGOA/DMAB for two different wavelengths 514.5 nm (a) and 488 nm (b).

build-up as is evidenced by an appearance of a light self-diffraction. The kinetics of grating formation has been studied at two wavelengths of Ar^+ laser 514.5 and 488 nm by monitoring the first order diffracted beam's power. Fig. 13 shows obtained results—time dependence of the first-order diffraction efficiency for investigated material.

As can be seen from the plot presented in Fig. 13(a), one can notice that both polarisation configurations used enable grating recording at 514.5 nm. The grating of the type VV gives stronger diffraction than the VH (i.e. polarisation grating) one. Taking into account the shapes of obtained grating build-up curves one notices that they are different from typical ones [25,26]. Usually diffraction signal build-up increases gradually with time until saturation is reached. In the present case two stages are observed. Initially the grating of the both VH and VV type gives high diffraction in relatively short time after beam opening and then the value of diffraction power decreases and starts growing again. The samples have been irradiated with laser light of 488 nm (VV polarisation) with various light powers: 6.05 and 13.5 mW (Fig. 13(b)). As can be seen from Fig. 13(b) the light intensity influences significantly the grating build-up process. For lower light powers the significance of the initial spike is reduced. The explanation of origin of the spike needs more detailed investigations, which are in progress.

4. Conclusion

The new diamine with azobenzene group has been utilized as curing agent of trifunctional aminophenol epoxy resin. Detailed IR investigations of the structural changes, which take place during the cure reactions, are carried out. The region of 922–878 cm^{-1} is chosen for quantitative studies of changes in the areas of the most characteristic bands changing in the reaction, namely absorption bands characteristic for vibration of amine and epoxy groups. It has been found that at temperature 190 °C only slight amount of epoxy group is present and it disappears completely after heating to 240 °C.

The curing kinetics has been studied using DSC

isothermal measurements. The model proposed by Kamal extended by the introduction of a diffusion factor let us describe kinetics of the cure reaction in the whole range of alfa. The good correlation between calculated data and experimental ones is obtained. This indicates that such kinetic models can be used to predict the chemical conversion that can be achieved in given conditions.

The dependence of glass transition temperature from conversion is examined. The presence of azobenzene groups in such epoxy systems enables their application as potential material for holography. Further study of kinetics of holographic grating recording and mechanism of grating formation in this novel polymer material is in progress.

References

[1] Shieh J-Y, Wang Ch-SJ. Polym Sci Polym Chem Ed 2002;40:369.
[2] Lee H, Neville K. Handbook of epoxy resins. New York: McGraw-Hill; 1976.
[3] Viswanathan NK, Kim DY, Bian S, Williams J, Liu W, Li L, Samuelson L, Kumar J, Triphaty SK. J Mater Chem 1999;9:1941.
[4] Kim DY, Triphaty SK, Li L, Kumar J. Appl Phys Lett 1995;66:1166.
[5] Triphaty S, Kim D-Y, Li L, Kumar J. Dev Technol 1998;34.
[6] Kim DY, Li L, Jiang XL, Shivshankar V, Kumar J, Triphaty SK. Macromolecules 1995;28:8835.
[7] Lee TS, Kim D-Y, Jiang XL, Kumar J, Triphaty SK. J Polym Sci Polym Chem Ed 1998;36:283.
[8] Mandal BK, Jeng RJ, Kumar J, Triphaty SK. Macromol Chem Rapid Commun 1991;12:607.
[9] Mija A, Casaval CN, Stoica Gh, Rosu D, Simonescu BC. Eur Polym J 1996;32:779.
[10] Horie K, Hiura H, Sawada M, Mita I, Kambe H. J Polym Sci Polym Chem Ed 1970;8:1357.
[11] Keenan MR. J Polym Sci Polym Chem Ed 1987;33:1725.
[12] Jungang G, Deling L, Shigang S, Guodong L. J Polym Sci Polym Chem Ed 2002;83:1586.
[13] Chern C-S, Poehlein W. Polym Engng Sci 1987;27:788.
[14] Opalicki M, Kenny JM, Nicolais L. J Polym Sci Polym Chem Ed 1996;61:1025.
[15] Wisanrakkit G, Gillham JK. J Appl Polym Sci 1990;41:2885.
[16] Wang X, Gillham JK. J Polym Sci Polym Chem Ed 1993;47:425.
[17] Wang X, Gillham JK. J Polym Sci Polym Chem Ed 1992;45:2127.
[18] Venditti RA, Gillham JK. J Appl Polym Sci 1997;64:3.
[19] Simon SL, Gillham JK. J Appl Polym Sci 1993;47:461.
[20] Abuin SP, Pellin MP, Nunez l, Gandara JS, Losada PP. J Appl Polym Sci 1993;47:533.
[21] Noël P, Roeges G. A guide to the complete interpretation of infrared spectra of organic structures. Chichester: Wiley; 1994. p. 248.
[22] Cole KC, Hechler J-J, Noel D. Macromolecules 1991;24:3098.
[23] Rabinowitch E. Trans. Faraday Soc. 1936;33:1225.
[24] Eichler HJ, Gunter P, Pohl D. Laser-induced dynamic gratings. Berlin: Springer; 1986.
[25] Sęk D, Schab-Balcerzak E, Sołyga M, Miniewicz A. Synth Met 2001; 9123:1.
[26] Schab-Balcerzak E, Grabiec E, Sęk D, Miniewicz A. Polym J 2003; 35:1.